J|A|C|S
ARTICLES
Published on Web 02/19/2003

Effects of As(III) Binding on α-Helical Structure

Daniel J. Cline, Colin Thorpe, and Joel P. Schneider*

Contribution from the Department of Chemistry and Biochemistry, University of Delaware, Newark, Delaware 19716-2522

Received August 23, 2002 ; E-mail: schneijp@udel.edu

Abstract: As(III) displays a wide range of effects in cellular chemistry. Surprisingly, the structural consequences of arsenic binding to peptides and proteins are poorly understood. This study utilizes model α-helical peptides containing two cysteine (Cys) residues in various sequential arrangements and spatial locations to study the structural effects of arsenic binding. With *i*, and $i + 1$, $i + 2$, or $i + 3$ arrangements, CD spectroscopy shows that As(III) coordination causes helical destabilization when Cys residues are located at central or C-terminal regions of the helix. Interestingly, arsenic binding to *i*, $i + 3$ positions results in the elimination of helical structure and the formation of a relatively stable alternate fold. In contrast, helical stabilization is observed for peptides containing *i*, $i + 4$ Cys residues, with corresponding pseudo pairwise interaction energies (ΔG_{pw}°) of -1.0 and -0.7 kcal/mol for C-terminal and central placements, respectively. Binding affinities and association rate constants show that As(III) binding is comparatively insensitive to the location of the Cys residues within these moderately stable helices. These data demonstrate that As(III) binding can be a significant modulator of helical secondary structure.

Introduction

Arsenic (III) species exert a wide array of effects in biological systems in part because of selective interactions with vicinal thiols in proteins and peptides. For example, inorganic As(III) derivatives ingested directly, or generated in vivo, can be both acute or chronic toxicants.[1−3] Although certain arsenic species are classified as human carcinogens, some have a venerable history as chemotherapeutics: for example, in Ehrlich's treatment of trypanosomiasis (e.g., African Sleeping Sickness).[4,5] Recently, arsenic trioxide (As_2O_3) has been used in the treatment of acute promyelocytic leukemia, perhaps via the induction of apoptosis.[6,7] In some cases, apoptosis may result from the binding of As(III) to proteins within the mitochondrion.[8] There are, however, many other potential intracellular and extracellular targets for arsenic attack.[9] Among these, several enzymes that utilize redox-active disulfides are susceptible including lipoamide dehydrogenase,[10,11] glutathione reductase,[12−14] and thioredoxin reductase.[15] Arsenic binding also impacts proteins involved in signaling pathways.[6,16]

In addition to these cellular effects, increasing emphasis is being placed on the design of organoarsenicals as probes of protein structure and function. Radiolabeled[17,18] or biotinylated[19,20] conjugates have been synthesized to monitor changes in the redox status of proteins carrying vicinal dithiols. An interesting example is the use of biarsenical fluorescein derivatives to label proteins containing an introduced sequence rich in Cys residues, namely, −Cys−Cys−Xaa−Xaa−Cys−Cys− (Xaa = any amino acid except cysteine).[21] That study, and its subsequent iteration,[22] underscores the need to clearly understand the conformational restraints imposed by As(III) coordination on protein structure. Thus, despite the plethora of biological effects of As(III), the multitude of cellular targets, and the recent advances in arsenic-based probe design, surprisingly little is known concerning the structural consequences of arsenic binding. This extends to the simplest case: the binding of monomeric arsenic species to simple dicysteine-containing peptides. A clearer understanding of these binding events may

(1) Hughes, M. F. ***Toxicol. Lett.*** **2002**, *133*, 1−16.
(2) Thomas, D. J.; Styblo, M.; Lin, S. *Toxicol. Appl. Pharmacol.* **2001**, *176*, 127−144.
(3) Vahter, M.; Concha, G. *Pharmacol. Toxicol.* **2001**, *89*, 1−5.
(4) Burri, C.; Nkunhu, S.; Merolle, A.; Smith, T.; Blum, J.; Brun, R. *Lancet* **2000**, *355*, 1419−1425.
(5) Friedheim, E. A. H. *Am. J. Tropical Medicine* **1949**, *29*, 173−180.
(6) Bode, A.; Dong, Z. G. *Drug Resistance Updates* **2000**, *3*, 21−29.
(7) Wang, Z. Y. *Cancer Chemother. Pharmacol.* **2001**, *48*, S72−S76.
(8) Larochette, N.; Decaudin, D.; Jacotot, E.; Brenner, C.; Marzo, I.; Susin, S. A.; Zamzami, N.; Xie, Z. H.; Reed, J.; Kroemer, G. *Exp. Cell Res.* **1999**, *249*, 413−421.
(9) Webb, J. L. *Enzymes and Metabolic Inhibitors*; New York, 1966; Vol. 3.
(10) Stevenson, K. J.; Hale, G.; Perham, R. N. *Biochemistry* **1978**, *17*, 2189−2192.
(11) Williams, C. H. *Lipoamide dehydrogenase, glutathione reductase, thioredoxin reductase, and mercuric ion reductase. A family of flavoenzyme transhydrogenases*; CRC Press: Boca Raton, FL, 1992; Vol. 3.
(12) Styblo, M.; Serves, S. V.; Cullen, W. R.; Thomas, D. J. *Chem. Res. Toxicol.* **1997**, *10*, 27−33.
(13) Chouchane, S.; Snow, E. T. *Chem. Res. Toxicol.* **2001**, *14*, 517−522.
(14) Muller, S.; Walter, R. D.; Fairlamb, A. H. *Mol. Biochem. Parasitol.* **1995**, *71*, 211−219.
(15) Lin, S.; Cullen, W. R.; Thomas, D. J. *Chem. Res. Toxicol.* **1999**, *12*, 924−930.
(16) Bode, A. M.; Dong, Z. G. *Crit. Rev. Oncology Hematology* **2002**, *42*, 5−24.
(17) Gitler, C.; Zarmi, B.; Kalef, E. *Anal. Biochem.* **1997**, *252*, 448−55.
(18) Gitler, C.; Mogyoros, M.; Kalef, E. *Labeling of Protein Vicinal Dithiols − Role of Protein-S-2 to Protein-(SH)(2) Conversion in Metabolic-Regulation and Oxidative Stress*, 1994; Vol. 233, pp 403−415.
(19) Donoghue, N.; Yam, P. T. W.; Jiang, X. M.; Hogg, P. J. *Protein Sci.* **2000**, *9*, 2436−2445.
(20) Donoghue, N.; Hogg, P. J. *Characterization of redox-active proteins on cell surface*, 2002; Vol. 348, pp 76−86.
(21) Griffin, B. A.; Adams, S. R.; Tsien, R. Y. *Science* **1998**, *281*, 269−272.
(22) Adams, S. R.; Campbell, R. E.; Gross, L. A.; Martin, B. R.; Walkup, G. K.; Yao, Y.; Llopis, J.; Tsien, R. Y. *J. Am. Chem. Soc.* **2002**, *124*, 6063−6076.

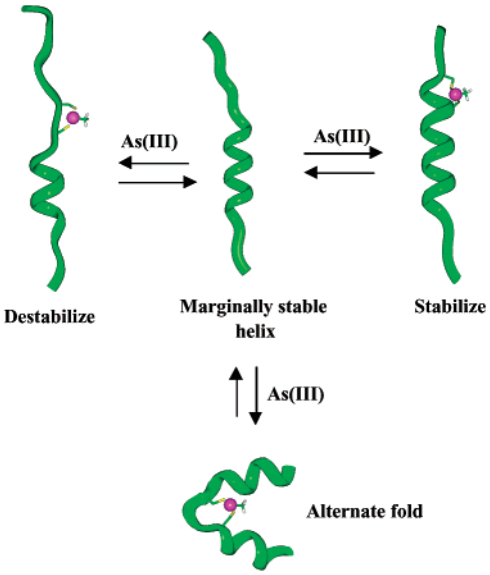

Figure 1. Schematic representation of As(III) binding to a marginally stable helical peptide containing two cysteine residues. Helix stabilization or destabilization leading to random coil or alternate conformations depends on the sequential arrangment of the cysteine residues.

assist in the design of more effective enzyme inhibitors, therapeutic agents, and probes.

In this paper, we investigate the effects of As(III) binding on the structure of dicysteine-containing α-helices, Figure 1. In most cases, arsenic binding to two Cys residues positioned within a model α-helix is a destabilizing event, leading to either an enhanced population of the random coil state or the formation of alternate folds. However, α-helices displaying cysteines at *i*, $i + 4$ positions will bind As(III) resulting in helical stabilization. This is somewhat surprising, since we find that disulfide bond formation between comparable cysteine residues is detrimental to helical structure.

Results and Discussion

Design Considerations. The effects of As(III) binding on helical structure can be assessed by monitoring the helical content of dicysteine-containing model helices as a function of arsenic concentration. We have prepared a family of peptides that incorporate two Cys residues at the *i*, and $i + 1$, $i + 2$, $i + 3$, or $i + 4$ positions of a model helix. These sequential arrangements have been chosen because of their relevance to dicysteine-containing sequences found in natural proteins. A query of the *Homo sapiens* proteome for the occurrence of dicysteine motifs indicates that there are 14 634 sequences containing one or more *i*, $i + 3$ motifs. In addition, 12 927, 11 930, and 12 418 sequences contain at least one copy of the *i* and $i + 1$, $i + 2$, and $i + 4$ motifs, respectively. Here, pairs of Cys residues have been placed at either the C-terminal end or middle of the helix resulting in peptides **1**−**4** and **5**−**8**, respectively (Table 1). These two sets of peptides allow one to study how different helical regions influence As(III) binding and the corresponding structural consequences of the binding event. Peptides **1**−**8** are designed to adopt marginally stable α-helices in aqueous solution and contain sequences based on the polyalanine model helices originally described by Baldwin.[23] These model peptides are monomeric in aqueous solution and their helical content has been shown to be highly responsive to side chain mediated metal binding events.[24]

The introduction of arsenic into peptides **1**−**8** is mediated by methyldiiodoarsine (H_3CAsI_2). This compound undergoes rapid hydrolysis in aqueous buffered solution to afford methylarsonous acid ($H_3CAs(OH)_2$).[25] Organoarsonous acids form three-coordinate As(III) complexes with dithiols forming intramolecular cyclic chelates[19] and are shown herein to bind to peptides **1**−**8** in a unimolecular fashion, Figure 1. Importantly, circular dichroism (CD) spectroscopy is used as the primary tool for observing secondary structural changes upon metal binding; we have found that methylarsonous acid displays minimal absorbance in the far UV and therefore should not contribute to the far UV−CD signal.

Structural Effects of As(III) Binding. Figure 2 shows CD spectra for each of the peptides in the presence and absence of one equivalent of methylarsonous acid. Apo-peptides **1**−**4**, incorporating Cys residues at the C-termini, display spectra that are characteristic of marginally stable α-helices (Figure 2a−d); a maximum at 190 nm because of helical contributions and minima at 200 and 222 nm because of random coil/helix and helix contributions, respectively, are observed. A recent report indicates that the random coil state of peptides rich in alanine at low temperature may actually contain a large degree of polyproline II structure.[26] Here, we are concerned with the effects of As(III) binding on α-helical structure regardless of what conformations actually populate the "random coil" state.

Upon binding As(III), peptides **1** and **2** display spectra consistent with an increase in population of random coil at the expense of helicity, Figure 2a and b. Interestingly, the spectrum of the peptide **3**−As(III) adduct is neither consistent with α-helical nor random coil structure and suggests that an alternate fold may be populated, Figure 2c. The spectrum can be classified as a class B′ type spectrum, typical for several classes of reverse turns.[27] This is an exciting possibility in that metal-based conformational switches for helix-turn transformations may find use in sensor and environmentally responsive biomaterial design. Figure 2d shows that peptide **4** is capable of binding As(III) resulting in the stabilization of existing helical structure. These data show that at the helix C-terminus, *i*, and $i + 1$, $i + 2$, or $i + 3$ arranged Cys residues bind As(III) resulting in the destabilization of the fold. In contrast, an *i*, $i + 4$ arrangement leads to helical stabilization.

CD was also used to verify the 1:1 stoichiometry of the As(III) binding event. Figure 3 shows data in which peptides **2** and **4** were titrated with methylarsonous acid, and $[\theta]_{222}$ was monitored as a function of added metal. The data, representative of peptides **1**−**8**, clearly show that this class of peptides bind arsenic in a 1:1 fashion regardless of whether helix destabilization (peptide **2**) or stabilization (peptide **4**) results. MALDI-TOF mass spectroscopy of As(III)-bound peptides confirm this mode of binding (see Supporting Information).

Peptides **5**−**8**, incorporating Cys residues in the central portion of the helix, behave similarly. In the absence of As-

(23) Marqusee, S.; Baldwin, R. L. *Proc. Natl. Acad. Sci. U.S.A.* **1987**, *84*, 8898−8902.
(24) Ruan, F. Q.; Chen, Y. Q.; Hopkins, P. B. *J. Am. Chem. Soc.* **1990**, *112*, 9403−9404.
(25) Gailer, J.; Madden, S.; Cullen, W. R.; Denton, M. B. *Appl. Organomet. Chem.* **1999**, *13*, 837−843.
(26) Shi, Z. S.; Olson, C. A.; Rose, G. D.; Baldwin, R. L.; Kallenbach, N. R. *Proc. Natl. Acad. Sci. U.S.A.* **2002**, *99*, 9190−9195.
(27) Smith, J. A.; Pease, L. G. *CRC Crit. Rev. Biochem.* **1980**, *8*, 315−399.

Table 1

peptide	sequence	DiCys position	% helix apo-peptide	% helix MeAs-peptide	ΔG_{pw}° (kcal/mol)	K_d (nM)	K_{on} ($M^{-1}s^{-1}$)
1	Ac−YGGKAAAAKA AAAKA**CC**A-NH_2	*i*, *i* + 1	20.8	14.3		74 (12)	14430 (230)
2	Ac−YGGKAAAAKA AAAK**C**A**C**A-NH_2	*i*, *i* + 2	18.6	4.2		30 (19)	10970 (110)
3	Ac−YGGKAAAAKA AA**C**KA**C**AA-NH_2	*i*, *i* + 3	16.8	n/a		50 (20)	14250 (140)
4	Ac−YGGKAAAAKA AA**C**KAA**C**A-NH_2	*i*, *i* + 4	18.7	32.0	−1.0	198 (55)	14080 (120)
5	Ac−YGGKAAAAKA **CC**AKAAAA-NH_2	*i*, *i* + 1	5.5	n/a		130 (19)	27670 (210)
6	Ac−YGGKAAAAK**C** A**C**AKAAAA-NH_2	*i*, *i* + 2	6.8	n/a		15 (10)	21580 (290)
7	Ac−YGGKAAACKA **C**AAKAAAA-NH_2	*i*, *i* + 3	7.8	n/a		88 (27)	23910 (300)
8	Ac−YGGKAAA**C**KA A**C**AKAAAA-NH_2	*i*, *i* + 4	9.6	20.6	−0.7	28 (6)	26550 (540)
9	Ac−YGGKAAAAKA AAAKAAAA-NH_2		56.9				

(III), these peptides exist in a coil-helix equilibrium that highly favors coil, Figure 2e−h. This is due to replacing Ala residues (having high helical propensity) with lower propensity Cys residues in the center of the helix as opposed to the ends (peptides **1**−**4**) where end-fraying already destabilizes the fold. The addition of As(III) results in helix destabilization for peptides **5**−**7** and stabilization of peptide **8**. Again peptide **7**, having *i*, *i* + *3* Cys residues, adopted an alternate structure upon arsenic binding resulting in a CD spectrum that can be classified as type B′ (compare Figure 2c and g). Last, the CD spectra of control peptide **9** (which is void of Cys residues) in the presence and absence of As(III) are identical indicating that the spectral changes observed for the other peptides result from arsenic binding to Cys residues within the sequence (see Supporting Information).

Collectively, these data suggest that helical regions of proteins containing two Cys residues in almost all of the common local sequential arrangements are susceptible to structural destabilization via arsenic binding. In contrast, one can expect that Cys residues at *i*, *i* + 4 positions, whether at the C-terminal end or middle of a helix, will bind As(III) resulting in helical stabilization.

Quantitative assessment of arsenic's ability to stabilize peptides **4** and **8** was accomplished by calculating pseudo pairwise interaction energies (ΔG_{pw}°) between the Cys side chains upon arsenic binding. Calculations were performed using a Lifson−Roig formalism modified to account for side-chain−side-chain interactions.[28] The helical content of both peptides **4** and **8** increases upon the addition of arsenic with corresponding ΔG_{pw}°'s of − 1.0 and −0.7 kcal/mol, respectively. Since favorable side-chain pairwise interactions enhance helix formation not only locally but over the entire length of the helix, As(III) binding might find general use in protein design to stabilize helical folds.

Intuitively, one might expect that both the *i*, *i* + 3 and *i*, *i* + 4 sequential arrangements of Cys residues would bind As(III) leading to helical stabilization. Thus, when contained in a segment of helix, the Cys residues in both arrangements appear close enough to bind As(III) via their side chains without any perturbation to helical main-chain dihedrals. Molecular modeling was used to gain insight into the possible binding modes of As(III) to Cys residues positioned in both arrangements. Figure 4 shows a depiction of the C-terminal portion of an energy-minimized model of peptide **4** (*i*, *i* + 4 arrangement) bound to methyl arsenite. The Cys side chains adopt trans and gauche (+) conformations for the N- and C-terminal residues, respectively. Statistical analysis of Cys side-chain rotamers found in helical segments of globular proteins indicate that these two rotamers are the most favored.[29] Also, the measured S−As−S bond angle of 102.9° in the model is consistent with the angles observed in the crystal structures of small methyl arsenite complexes.[30] Although As(III) binding to *i*, *i* + 3 Cys residues within a helix should be possible, modeling shows that the C-terminal Cys side chain must adopt a *gauche* (−) conformation, the least populated rotamer found in helical protein structure (model not shown).[29] These modeling experiments support the CD data and show that Cys side-chain rotamers conducive for helical structure are only accommodated in an *i*, *i* + 4 arrangement in the arsenic-bound state. In fact, we find that As(III) binding to peptides **3** and **7**, both having *i*, *i* + 3 Cys arrangements, results in the apparent total loss of helical structure and the population of an alternate fold, Figure 2c and 2g.

Although the CD spectrum of this alternate fold is consistent with several types of turn secondary structure,[27] detailed NMR studies are needed to investigate this possibility. In the interim, thermal-dependent CD spectroscopy was used to investigate the structural stability of this alternate fold. Figure 5 shows a thermal denaturation experiment in which the CD spectrum of the peptide **7**−As(III) adduct was monitored as a function of temperature. This metal-induced fold is stable up to 50 °C, an unexpected degree of stability for such a small peptide.

One might expect that arsenic ligation and intramolecular disulfide bond formation should exert comparable effects on helical structure. We have studied the effect of intramolecular disulfide bond formation on helical structure using peptides **1**−**8**. Interestingly, disulfide bond formation within each peptide resulted in a loss of helical content, even when formed between Cys residues in an *i*, *i* + 4 arrangement (data not shown). This suggests that the preferred dihedral geometries of the cystine S−S bond are not conducive with helical structure but that the incorporation of one additional atom (e.g., As(III)) affords a greater degree of conformational freedom within the cross-link and leads to side-chain rotamers that favor helical structure.

Chelate Stability and Kinetics. Investigations into the kinetics of metal complexation and the stability of the resultant chelate are most easily accomplished spectrophotometrically. To this end, we have designed a simple arsenic probe that displays a distinct absorbance profile when bound to peptides **1**−**8**.

p-Succinylamidephenyl arsenoxide (PSAO), prepared from the ring opening of succinic anhydride with *p*-aminophenyl arsenoxide, proved to be an easily prepared, highly water soluble, and traceable means of delivering As(III).

(28) Stapley, B. J.; Rohl, C. A.; Doig, A. J. *Protein Sci.* **1995**, *4*, 2383−2391.
(29) McGregor, M. J.; Islam, S. A.; Sternberg, M. J. E. *J. Mol. Biol.* **1987**, *198*, 295−310.
(30) Dimaio, A. J.; Rheingold, A. L. *Inorg. Chem.* **1990**, *29*, 798−804.

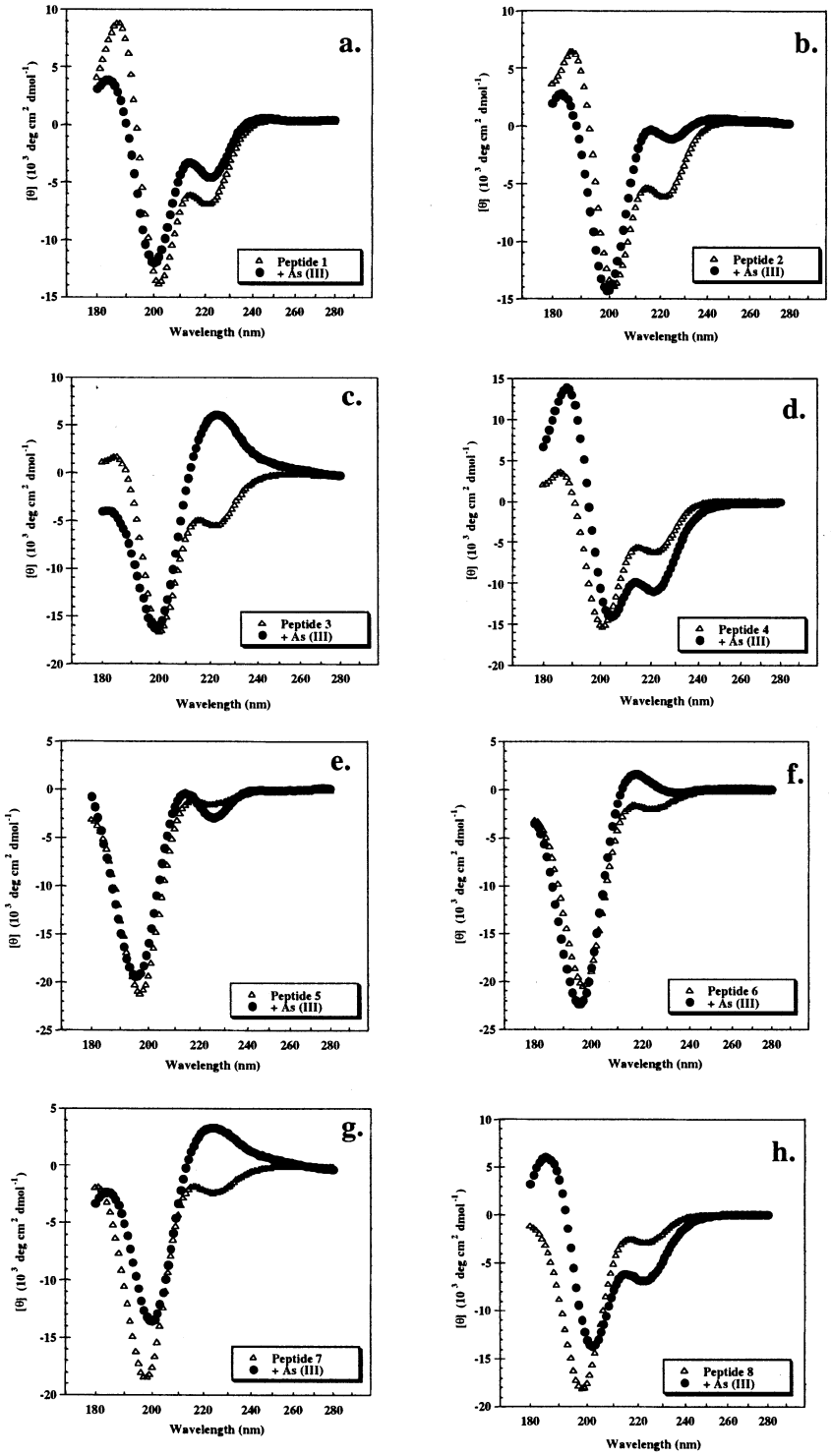

Figure 2. Far UV−CD spectra of 100 μM solutions of peptides (pH 7.0, 5 mM potassium phosphate, 15 mM KF) at 2 °C in the absence and presence of one equivalent $H_3CAs(OH)_2$.

Figure 6a shows an absorption spectrum of bound PSAO that is significantly red-shifted compared to that of free PSAO. Accordingly, the absorbance at 300 nm can be conveniently monitored in a spectrophotometric titration, such as that shown in panel b for peptide **4**, affording data suitable for K_d determination. The same wavelength is used in panel c to follow the kinetics of the binding reaction of peptide **4** with PSAO by stopped-flow spectrophotometry. The data are fit to a single exponential and the inset in panel c shows that the reaction is second-order overall judged by the linear dependence of the apparent rate constant on PSAO concentration. The remaining peptides were analyzed as in Figure 6 (see Supporting Information) and the data collected in Table 1 (associated errors are shown in parentheses). Despite the differences observed in the CD data for peptides **1**−**8** upon As(III) binding, there is little difference in dissociation constants, and relatively tight binding was seen throughout (30−200 nM). This suggests that the sequential arrangement of the Cys residues and their location

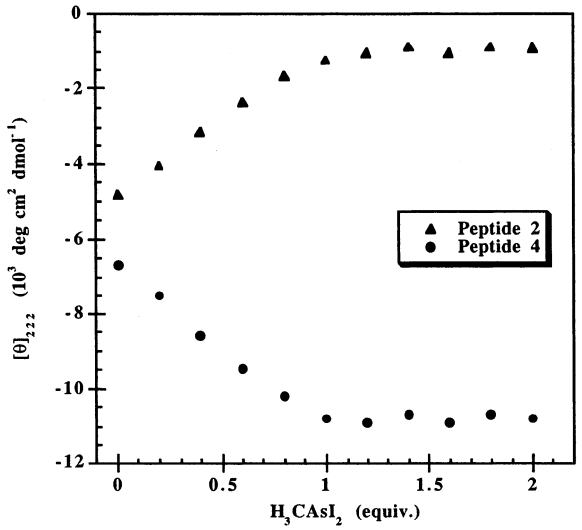

Figure 3. Arsenic titration of 15 μM solutions of peptides **2** and **4** (pH 7.0, 5 mM BTP, 15 mM NaCl, 0.15 mM TCEP) monitoring $[\theta]_{222}$ as a function of added metal at 2 °C. A 1:1 binding stoichiometry, further confirmed by MALDI-TOF MS, is observed for peptides **1**−**8**.

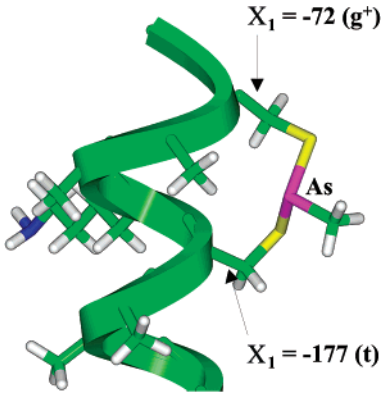

Figure 4. Depiction of the C-terminal region of an energy-minimized model (Discover3) of peptide **4** bound to methyl arsenite. The measured χ_1 angles ($C_\alpha-C_\beta$ bonds) of the N- and C-terminal cysteines are consistent with trans and gauche (+) conformations as defined by McGregor,[29] respectively. These conformations are statisically preferred for cysteine residues found in helical regions of globular proteins.

within the helix are relatively unimportant for tight binding regardless of the structural consequences of the binding event. A small difference in association rate constants is evident among the peptides containing Cys residues in the middle versus the end of the helix. A possible explanation is that the Cys residues located in the central portion of the peptide adopt helical dihedrals conducive to metal binding. Cys residues at the ends of the peptide would experience end fraying leading to a slight increase in the activation entropy of metal binding. However, since there is less than a 3-fold difference in rate among all the peptides, such arguments are purely conjectural. Therefore, for most peptides containing spatially close Cys residues, one would expect As(III) to bind efficiently regardless of the structural outcome. It will be interesting to explore the consequences of arsenic binding to surface-exposed Cys residues in helical regions of native proteins.

Conclusions

Peptides containing two Cys residues in different sequential arrangements were prepared to investigate the effects of As(III) binding on moderately stable helical structure. In most cases, As(III) binding proved to be a potent driving force for the alteration of helical structure regardless of the sequential positioning of the Cys residues with respect to each other or their relative position within an α-helix. However, Cys residues contained at *i*, *i* + 4 positions of marginally stable helices will bind As(III) resulting in an enhancement of helical structure. Interestingly, As(III) binding of *i*, *i* + 3 Cys-containing helical peptides results in the total elimination of helical structure and the formation of an alternate fold that is quite stable to heat denaturation. This is an intriguing result when one contemplates the preponderance of proteins that contain Cys residues in this arrangement (many redox active proteins) and their possible role in arsenic induced apoptosis and toxicity. Finally, these results should be considered in the design of As(III) binding peptides and proteins, especially fusion proteins used in organoarsenic-based assays.

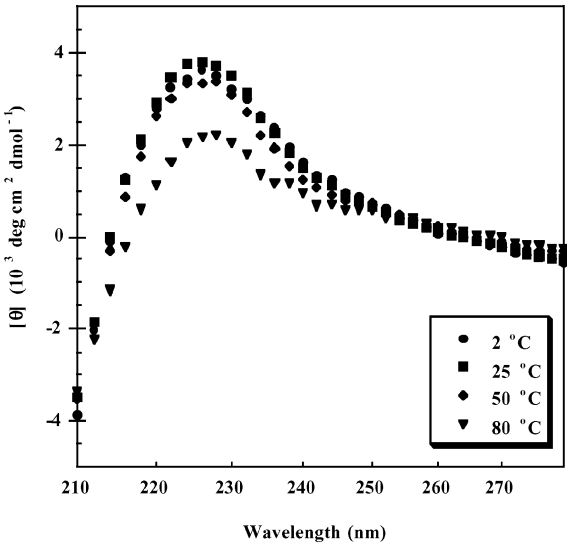

Figure 5. Temperature dependence of far UV−CD spectra for 100 μM solution of peptide 7 (pH 7.0, 5 mM BTP, 15 mM NaCl) in the presence of 1.0 equiv of $H_3CAs(OH)_2$.

Experimental Section

General Methods and Material. NOTE: Inorganic arsenic is classified as a human carcinogen and all species described herein should be treated with due caution. Trifluoroacetic acid (TFA), 1, 3-bis[tris-(hydroxymethyl)methylamino]propane (BTP), ethylenediaminetetraacetic acid (EDTA), piperidine, thioanisole, ethanedithiol, and anisole were purchased from Acros. Tris(2-carboxyethyl)phosphine hydrochloride (TCEP−HCl) was purchased from Pierce. Methyldiiodoarsine was prepared as described by Millar[31] and *p*-aminophenyl arsenoxide as described by Stevenson.[10] Fmoc Amide resin was purchased from Applied Biosystems. The appropriate side-chain protected Fmoc amino acids, 2-(1H-benzotriazole-1-yl)-1,1,3,3-tetramethyluronium hexafluorophosphate (HBTU), and 1-hydroxybenzotriazole (HOBT) were purchased from Novabiochem. All peptides were purified by RP-HPLC using a preparative Vydac C18 peptide/protein column and HPLC solvents consisting of solvent A (0.1% TFA in water) and solvent B (90% acetonitrile, 10% water, and 0.1% TFA). Molecular weights of peptides were determined by MALDI-TOF mass spectroscopy.

Synthesis of Peptides. Peptides **1**−**8** were prepared on Fmoc Amide resin via automated Fmoc peptide synthesis employing an ABI 433A peptide synthesizer and HBTU/HOBT activation. The resulting dry

(31) Millar, I. T.; Heaney, H.; Heinekey, D. M.; Fernelius, W. C. *Inorg. Synth.* **1960**, *6*, 113−115.

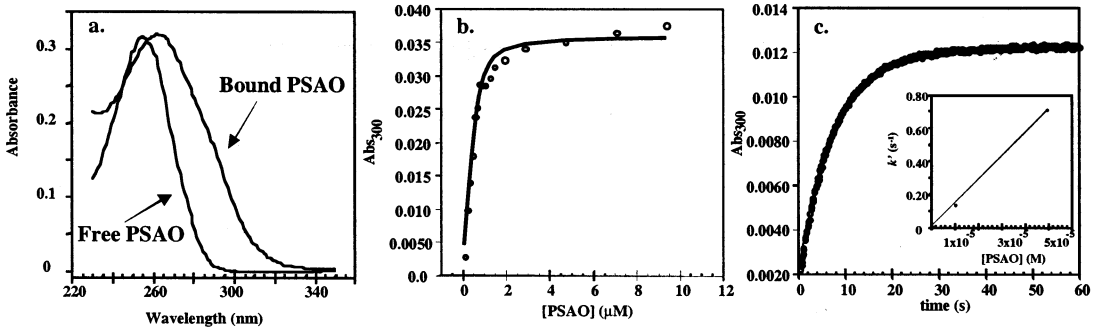

Figure 6. (a) Serial difference absorption spectra of free and peptide **4**-bound PSAO (0.25 μM, pH 7.0, 5 mM BTP, 15 mM NaCl, 0.03 mM EDTA) demonstrating that the absorbance at 300 nm can be used to conveniently monitor the formation of peptide-bound PSAO. (b) A_{300} vs PSAO concentration for a 1 μM solution of peptide **4** in a 5-cm cell; the data are fit to a 1:1 binding stoichiometry yielding a K_d of 198 nM. (c) Stopped-flow absorbance measurements of As(III) binding to a 2.5 μM (final) solution of peptide **4** in a 1-cm cell under pseudo-first-order conditions showing simple monophasic behavior. The inset shows the linear fit of apparent rate constant vs PSAO concentration affording a second-order rate constant of 14 080 $M^{-1}s^{-1}$.

resin-bound peptides were cleaved and side chain deprotected using TFA:thioanisole:ethanedithiol:anisole (90:5:3:2). Crude peptides were subsequently dissolved in 0.1 M ammonium acetate (pH 7.0, 1 mg/mL) containing 10 equiv TCEP and stirred under nitrogen for 1 h prior to purification. Purification by RP-HPLC employing a linear gradient from 5% to 18% B over 6 min, followed by an additional gradient from 18% to 28% B over 50 min resulted in pure, fully reduced peptides **1**−**8**. Mass spectroscopy: calculated molecular weights for **1**−**8** are identical $(M + H)^+ = 1637.8$; observed $(M + H)^+$, peptide **1**, 1637.8; peptide **2**, 1637.8; peptide **3**, 1637.9; peptide **4**, 1637.9; peptide **5**, 1637.6; peptide **6**, 1637.5; peptide **7**, 1637.7; peptide **8**, 1637.6; peptide **9**, 1574.1 [$(M + H)^+$, calcd 1573.9].

Synthesis of *p*-Succinylamidephenyl arsenoxide (PSAO). A 100-mL round-bottomed flask was charged with *p*-aminophenyl arsenoxide (2.0 g, 10.0 mmol) and 40 mL of acetone. This mixture was stirred for 0.5 h and any solid *p*-aminophenyl arsenoxide removed by filtration. The resulting solution was stirred and succinic anhydride (1.0 g, 10.0 mmol) was added at once as a solid. After stirring 24 h under nitrogen atmosphere, the resulting precipitate was collected by filtration, washed with copious amounts of diethyl ether, and dried under vacuum to afford 2.4 g of PSAO (8.0 mmol, 80%) as a white solid. ^{1}H NMR (CD_3OD, 400 MHz) δ 7.67 (d, $J = 8.6$ Hz, 2H), 7.56 (d, $J = 8.6$ Hz, 2H), 2.67 (m, 4H); ^{13}CNMR (CD_3OD, 400 MHz) δ 176.7, 173.4, 142.7, 141.2, 132.2, 121.0, 32.8, 30.3.

Circular Dichroism Studies. CD spectra were collected on an AVIV model 215 spectropolarimeter. Wavelength spectra of 100 μM solutions of peptides **1**−**8** (pH 7.0, 5 mM potassium phosphate, 15 mM KF) in the absence and presence of one equivalent of methylarsonous acid were obtained at 2 °C in a 1-mm quartz cell. Titration experiments were performed employing a 1-cm quartz cell and the instrument's autotitrator programmed to deliver successive additions (0.2 equiv) of methylarsonous acid from a concentrated aqueous stock (1 mM) to 15 μM solutions of peptide (pH 7.0, 5 mM BTP, 15 mM NaCl, 0.15 mM TCEP) at 2 °C. Peptide samples were prepared from stock solutions in water and diluted with the appropriate buffer. The concentration of peptide solutions was determined by Tyr absorbance at 276 nm ($\epsilon = 1450\ cm^{-1}\ M^{-1}$). Mean residue ellipticity $[\theta]$ was calculated using the equation $[\theta] = (\theta_{obs}/10lc)/r$, where θ_{obs} is the measured ellipticity in millidegrees, l is the length of the cell (cm), c is the concentration (M), and r is the number of residues. Percent helicity values are based on fraction helix (f_h) at 2 °C. Fraction helix was calculated according to Rohl and Baldwin[32] where $f_h = ([\theta]_{222} - 550)/([-42250(1 - 3/Nr)] - 550)$, where Nr is the number of residues in a helical conformation. Fraction helix values are accurate within 3%.[28] Initiation (v), propagation (w), n-capping (n), c-capping (c), and i, $i + 4$ side-chain pairwise interaction (p) parameters used for the determination of $\Delta G_{pw}°$ can be found in the Supporting Information. Assuming ±3% error in fraction helix values, standard error of the mean for values of p for peptides **4** and **8** are 0.029 and 0.006 and correspond to propagated error in $\Delta G_{pw}°$ of 3.1×10^{-3} and 1.0×10^{-3} kcal/ mole, respectively.

UV Spectroscopic Studies. Employing a 5-cm quartz cell, dissociation constants were determined by monitoring the change in absorbance at 300 nm of solutions of reduced peptide (pH 7.0, 5.0 mM BTP, 15 mM NaCl) upon the addition of 0.25 equiv aliquots of PSAO from an aqueous stock. The peptide concentration for each sample was determined via the extinction coefficient of the As(III)-bound peptide ($\epsilon_{300} = 6000\ cm^{-1}\ M^{-1}$). After each ligand addition, the solution was equilibrated for 15 min. EDTA (0.03 mM) was added to solutions of peptides prone to oxidation prior to ligand addition. Plots of absorbance versus concentration of PSAO were fit to eq 1 using Igor Pro where A = observed absorbance, A_o = absorbance of apopeptide, A_f = absorbance of peptide:ligand complex, P_t = total peptide concentration, K_d = dissociation constant, and L_t = total ligand concentration. At high total PSAO concentrations, free PSAO has a small contribution to the absorbance at 300 nm (which is not taken into account in eq 1) resulting in small incremental increases in the data above the fit line. Sensitivity analysis of the data indicates that this contribution does not effect the reported K_d beyond the errors reported in Table 1.

$$A = A_o + (A_f - A_o)\frac{(P_t + K_d + L_t) - \sqrt{(P_t + K_d + L_t)^2 - 4P_tL_t}}{2P_t} \quad (1)$$

Stopped-Flow Studies. A model SF-61 DX2 stopped-flow spectrometer (Hi-Tech Scientific) equipped with a 75 W superquiet Xenon lamp was used for stopped-flow kinetics experiments. Stock solutions of peptides **1**−**8** and PSAO (pH 7.0, 50 mM BTP, 150 mM NaCl, 0.3 mM EDTA) were mixed rapidly to give final concentrations of 2.5 μM in peptide and 10, 25, or 50 μM PSAO. Absorbance changes were monitored at 300 nm, and the data were fit to single-exponential equations using KinetAsyst 3 software. Averages of three of the resultant apparent rate constants were plotted versus PSAO concentration using Graphpad Prism 3.0 to calculate the overall second-order rate constants.

Proteome Data Base Query. The Protein Information Resource Reference Library (PIR, Georgetown University) was employed to search the *Homo sapiens* database for CXXXC, CXXC, CXC, and CC motifs. This database can be found on the WWW at http://pir.georgetown.edu/pirwww/search/pirnref.shtml.[33]

Acknowledgment. This work was funded in part by ACS PRF-G: 36376-G4 (JPS), NIH 26643 (CT) and by Training Grant USPHS 1-T32-GM08550 to D. C. We would like to thank Carol Rohl for helpful discussion.

(32) Rohl, C. A.; Baldwin, R. L. *Methods Enzymol.* **1998**, *295*, 1−26.

(33) Wu, C. H.; Huang, H. et al. *Nucleic Acids Res.* **2002**, *30*, 35−37.

Supporting Information Available: Index, representative HPLC, and mass spectroscopy data; CD-based As(III) titrations, K_d determinations, and associative rate data for all peptides; ΔG_{pw} determination for peptides 4 and **8**. This material is available free of charge via the Internet at http://pubs.acs.org. JA0282644